UNCLASSIFIED

AD 268 332

Reproduced
by the

ARMED SERVICES TECHNICAL INFORMATION AGENCY
ARLINGTON HALL STATION
ARLINGTON 12, VIRGINIA

UNCLASSIFIED

NOTICE: When government or other drawings, specifications or other data are used for any purpose other than in connection with a definitely related government procurement operation, the U. S. Government thereby incurs no responsibility, nor any obligation whatsoever; and the fact that the Government may have formulated, furnished, or in any way supplied the said drawings, specifications, or other data is not to be regarded by implication or otherwise as in any manner licensing the holder or any other person or corporation, or conveying any rights or permission to manufacture, use or sell any patented invention that may in any way be related thereto.

6-2-1-5
XEROX

CATALOGED BY ASTIA
AS AD No. 268332

268 332

ZPh-119
Physics Section

INFRARED EMISSIVITY OF DIATOMIC GASES WITH DOPPLER LINE SHAPE

W. Malkmus

September 1961

ASTIA
DEC 26 1961
TIPDR
A

GENERAL DYNAMICS | CONVAIR

ZPh-119
Physics Section

INFRARED EMISSIVITY OF DIATOMIC GASES WITH DOPPLER LINE SHAPE

W. Malkmus

September 1961

This work was conducted under
Geophysics Research Directorate
Air Force Cambridge Research Laboratories
Contract No. AF 19 (604)-5554
ARPA Order No. 116, Project Defender

GENERAL DYNAMICS | CONVAIR

INFRARED EMISSIVITY OF DIATOMIC GASES WITH DOPPLER LINE SHAPE

W. Malkmus

In a previous publication,[1] expressions were developed for the infrared emissivities of diatomic gases in the first approximation to the vibration-rotation interaction.

Computations were made previously in the weak line and strong line (Lorentz pressure-broadened line shape) approximation. The present work is an extension of the previous analysis to the case of a Doppler-broadened line shape, which is of particular importance at low pressures and long path lengths.

The equivalent width of an isolated line of integrated intensity S with Doppler shape is given by[2]

$$W^{s\ell} = SX \sum_{n=0}^{\infty} \frac{(-P' X)^n}{(n+1)! \sqrt{n+1}} \tag{1}$$

where

$$P' = \frac{S}{\omega_o} \sqrt{\frac{mc^2}{2\pi kT}} \tag{2}$$

and

$$X = p\ell \quad . \tag{3}$$

The average emissivity of an Elsasser band is given by

$$\epsilon = \frac{W^{s\ell}}{d} \quad , \tag{4}$$

where $W^{s\ell}$ and d are the equivalent line width and line spacing, if overlapping of the lines in the band is neglected. The average

emissivity of a number of randomly superposed Elsasser bands (random Elsasser model) is given by

$$\epsilon = 1 - \prod_{v} \left(1 - \frac{W_v^{s\ell}}{d_v}\right) . \tag{5}$$

For the anharmonic vibrating rotator model previously analyzed,[1] the average line strength $S_v^{v+1(\mp)}(\omega)$ at frequency ω for a $|\Delta v| = 1$ transition is given in terms of the total band absorption α_v^{v+1} by[1]

$$S_v^{v+1(\mp)}(\omega) = \frac{\alpha_v^{v+1} B_e hc}{\bar{\omega}_v^{v+1} kT} \omega \left| \frac{B_e - \alpha_e(v+1) \mp \sqrt{[B_e - \alpha_e(v+1)]^2 - \alpha_e(\omega - \omega_v)}}{\alpha_e} \right| x$$

$$\exp\left[\frac{-hc}{k\alpha_e^2 T}\left[B_e - \alpha_e(v+1)\right]\left\{2\left[B_e - \alpha_e(v+1)\right]\left[B_e - \alpha_e(v+1)\right.\right.\right.$$

$$\left.\left.\left. \mp \sqrt{[B_e - \alpha_e(v+1)]^2 - \alpha_e(\omega - \omega_v)}\right] - \left(1 + \frac{\frac{1}{2}\alpha_e}{B_e - \alpha_e(v+1)}\right)\alpha_e(\omega - \omega_v)\right\}\right] x$$

$$\left(1 + \frac{C}{\alpha_e}\left[B_e - \alpha_e(v+1) \mp \sqrt{[B_e - \alpha_e(v+1)]^2 - \alpha_e(\omega - \omega_v)}\right]\right)\left(1 - e^{\frac{-\omega hc}{kT}}\right), \tag{6}$$

where the upper sign refers to the main portion of the band and the lower sign to the returning R-branch. The quantity $\omega_v^{v'}$ is approximated by[1]

$$\bar{\omega}_v^{v'} = \omega_v \left[1 - \exp\left(-\frac{hc\omega_v}{kT}\right)\right] , \tag{7}$$

where

$$\omega_v = \omega_e - 2(v+1)\,\omega_e x_e + \left[3(v+1)^2 + \tfrac{1}{4}\right]\omega_e y_e + \left[4(v+1)^3 + (v+1)\right]\omega_e z_e . \tag{8}$$

The average line spacing at frequency ω is given by[1]

$$d_v(\omega) = 2\sqrt{[B_e - \alpha_e(v+1)]^2 - \alpha_e(\omega - \omega_v)} . \tag{9}$$

The total band strength at any temperature, $\alpha_v^{v+1}(T)$, can be approximated from an experimental value of the strength of any band

(usually the 0-1 band) at any other temperature by the expressions[1]

$$\frac{\alpha_v^{v+1}(T)}{\alpha_v^{v+1}(T_o)} = \frac{T_o}{T} \frac{\bar{\omega}_o^1(T)\ \bar{\omega}_v^{v+1}(T)}{\bar{\omega}_o^1(T_o)\bar{\omega}_v^{v+1}(T_o)} \exp\left[\left[E(v) - E(0,0)\right] \frac{hc}{k}\left(\frac{1}{T_o} - \frac{1}{T}\right)\right] \tag{10}$$

and

$$\frac{\alpha_{v'}^{v'+1}(T)}{\alpha_v^{v+1}(T)} = \frac{v' + 1}{v + 1} \exp\left[-\left(E(v') - E(v)\right)\frac{hc}{kT}\right] . \tag{11}$$

Equation (11) is based on the harmonic oscillator assumption.

The average emissivity at frequency ω for a number of superposed bands with Doppler line shape is given by

$$\epsilon_\omega = 1 - \prod_v \left[1 - \frac{W_v^{s\ell(-)}(\omega)}{d(\omega)}\right]\left[1 - \frac{W_v^{s\ell(+)}(\omega)}{d(\omega)}\right] , \tag{12}$$

where

$$W_v^{s\ell(\mp)} = S_v^{v+1(\mp)}\ X \sum_{n=o}^{\infty} \frac{(-P_v'^{(\mp)}\ X)^n}{(n+1)!\ \sqrt{n+1}} \tag{13}$$

and

$$P_v'^{(\mp)} = \frac{S_v^{v+1(\mp)}}{\omega_o} \sqrt{\frac{mc^2}{2\pi kT}} . \tag{14}$$

The summation in Equation (13) was computed for large values of its argument by use of the asymptotic expansion[2]

$$\sum_{n=o}^{\infty} \frac{(-y)^n}{(n+1)!\ \sqrt{n+1}} = \frac{2}{\sqrt{\pi}}\ \frac{1}{y}\left[\sqrt{\ell n\ y} + \frac{.2886}{\sqrt{\ell n\ y}} - \ldots\right] . \tag{15}$$

If the emissivity is of the order of a few percent or less, the approximation

$$\epsilon_\omega \approx \sum_v \frac{W_v^{s\ell(-)}(\omega) + W^{s\ell(+)}(\omega)}{d_v(\omega)} \qquad (16)$$

may be used.

The results of the evaluation of equation (16) for CO, NO, HCℓ, HF, and OH at temperatures of 1800, 3000, 5000, and 7000°K are shown in Figures 1 to 20 for values of pℓ ranging from 0.01 to 1000 atm-cm. It may be noted that the curve for 0.01 atm-cm in each case is virtually the same as that obtained by use of the weak line approximation, although a slight decrease is noticeable near the peaks.

The values of band strengths and line widths used are the same as those used previously.[1,3]

These curves may be used in conjunction with those computed in the strong line and weak line approximations to find approximate emissivities throughout the entire transition region from the weak line to the strong line approximation. The weak line approximation gives an upper limit to the emissivity while the Doppler shape approximation gives a lower limit. An approximation to the true emissivity can be obtained by an expression such as

$$\epsilon_\omega \approx \min \left[\epsilon_{WL}, \max (\epsilon_D, \epsilon_{SL}) \right] , \qquad (17)$$

where min and max mean the smaller and the larger respectively of their two arguments, and the subscripts WL, D, and SL refer to the weak line, Doppler, and strong line approximations, respectively.

For example, consider HF at T = 3000°K and ω = 3600 cm^{-1}, where the maximum emissivity of the P-branch occurs and the effect of saturation of the Doppler line shapeis most pronounced. For a fixed pressure of 0.01 atm, the average Lorentz half-width is about 0.00084 cm^{-1} as compared with the Doppler half-width of 0.016 cm^{-1}. For path lengths up to about

1000 cm the Doppler line shape predominates. (For path lengths of less than about 1 cm, however, ϵ_{WL} deviates from ϵ_D by less than 10%.) For path lengths greater than 1000 cm, ϵ_{SL} is greater than ϵ_D, and hence provides the better approximation.

For a pressure of 1 atm, the effect of the Doppler line shape is negligible. For $\ell \approx 0.5$ cm, ϵ_{WL} and ϵ_{SL} are equal; for shorter path lengths, ϵ_{WL} provides the best approximation and for greater lengths, ϵ_{SL} is the best.

For a pressure of 10^{-4} atm, ϵ_D is the best approximation for path lengths ranging up to about 10^7 cm, although for path lengths less than 100 cm, ϵ_{WL} is within 10% of ϵ_D.

ACKNOWLEDGMENT

The author wishes to acknowledge the assistance provided by Dr. A. Thomson in the original suggestion of this investigation as well as in subsequent discussions.

REFERENCES

1. W. Malkmus and A. Thomson, Convair Report ZPh-095, May 5, 1961; also in Journal of Quantitative Spectroscopy and Radiative Transfer (to be published).

2. G. N. Plass, J. Opt. Soc. Am. 48, 690 (1958).

3. W. Malkmus, Convair Report ZPh-120, September, 1961.

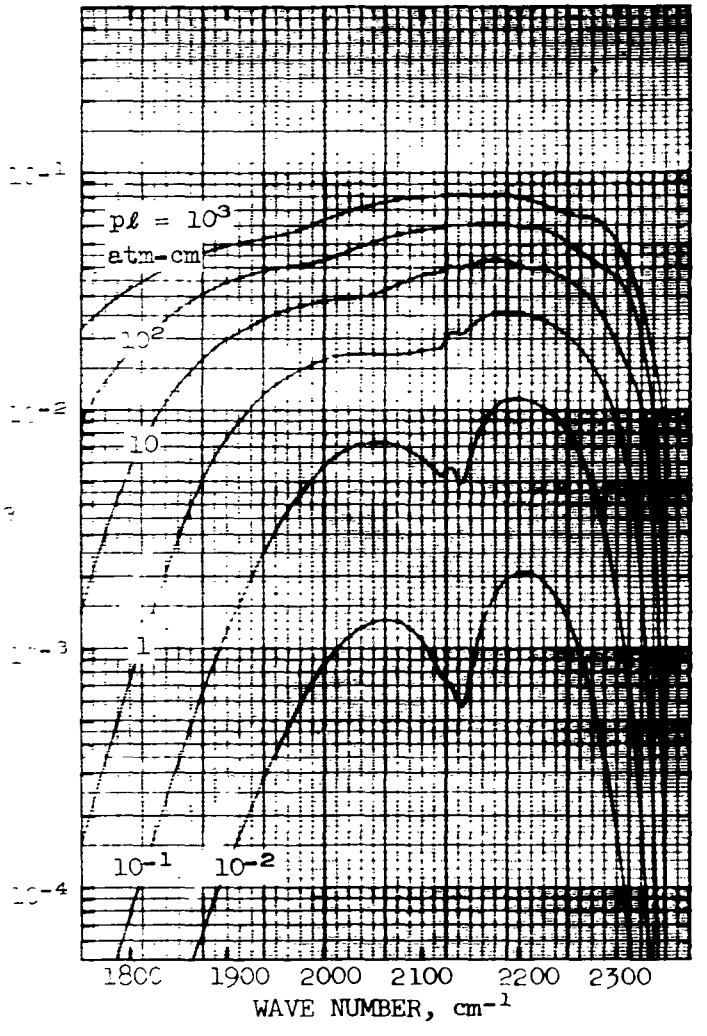

FIGURE 1. SPECTRAL EMISSIVITY OF CO AT T = 1800°K (Doppler Line Shape)

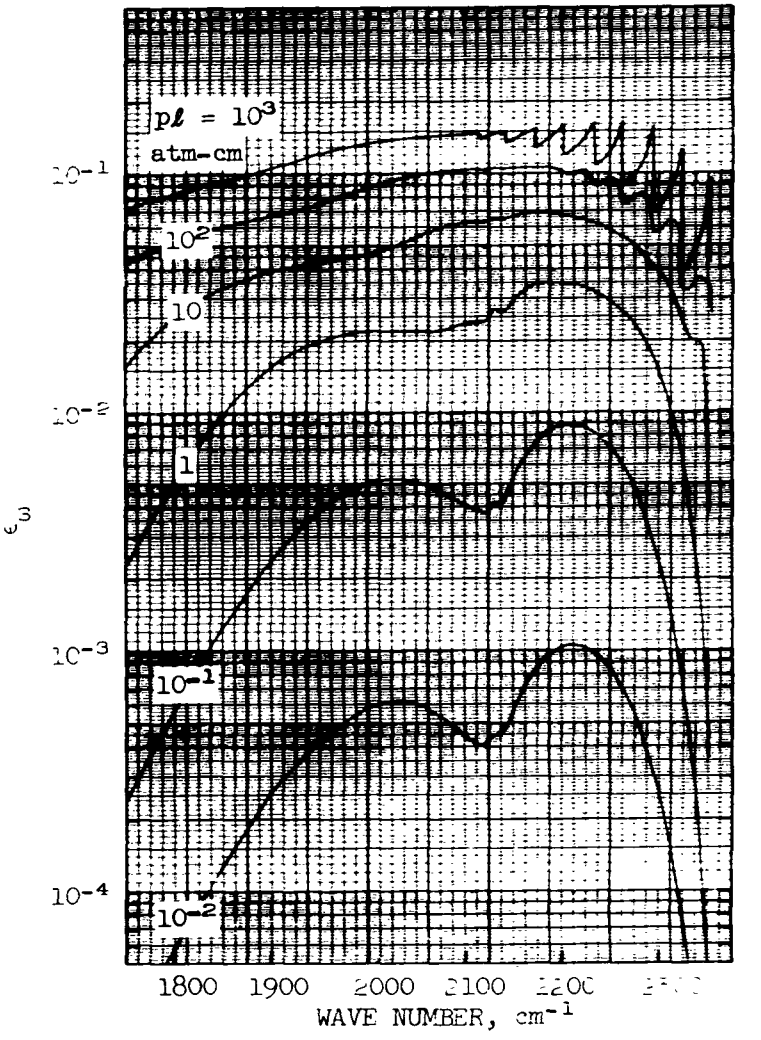

FIGURE 2. SPECTRAL EMISSIVITY OF CO AT T = 3000°K (Doppler Line Shape)

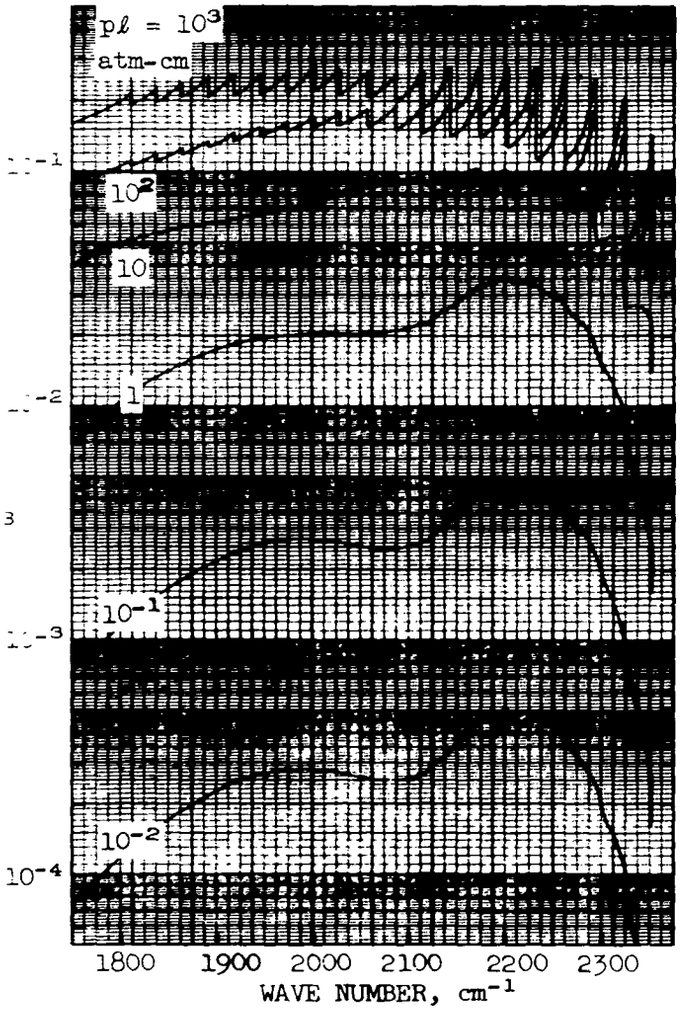

FIGURE 3. SPECTRAL EMISSIVITY OF CO AT T = 5000°K (Doppler Line Shape)

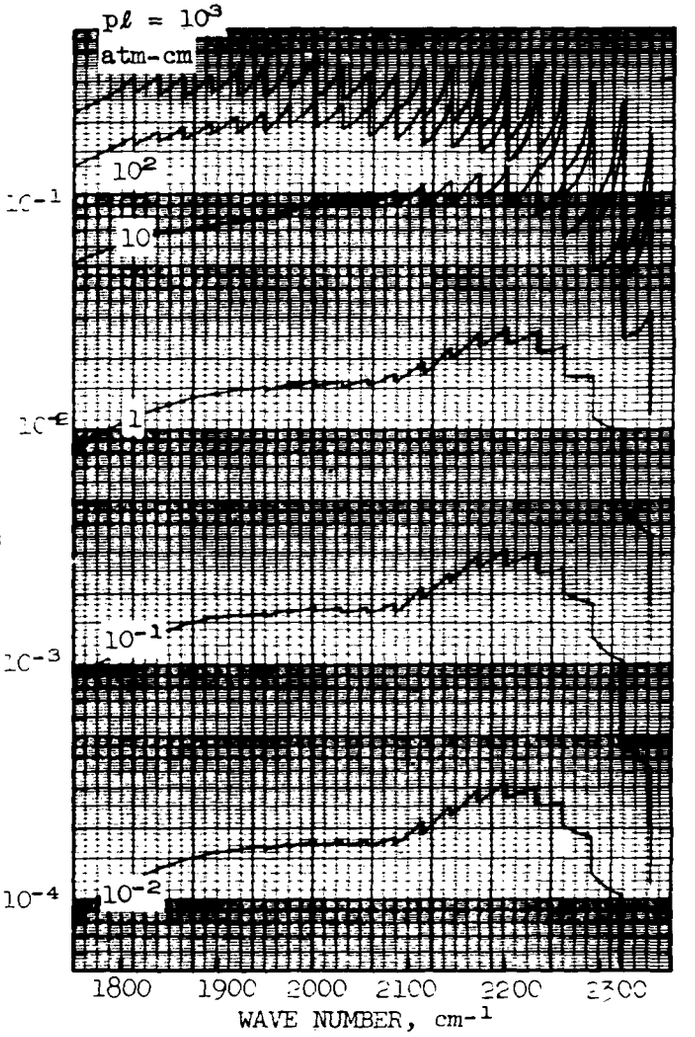

FIGURE 4. SPECTRAL EMISSIVITY OF CO AT T = 7000°K (Doppler Line Shape)

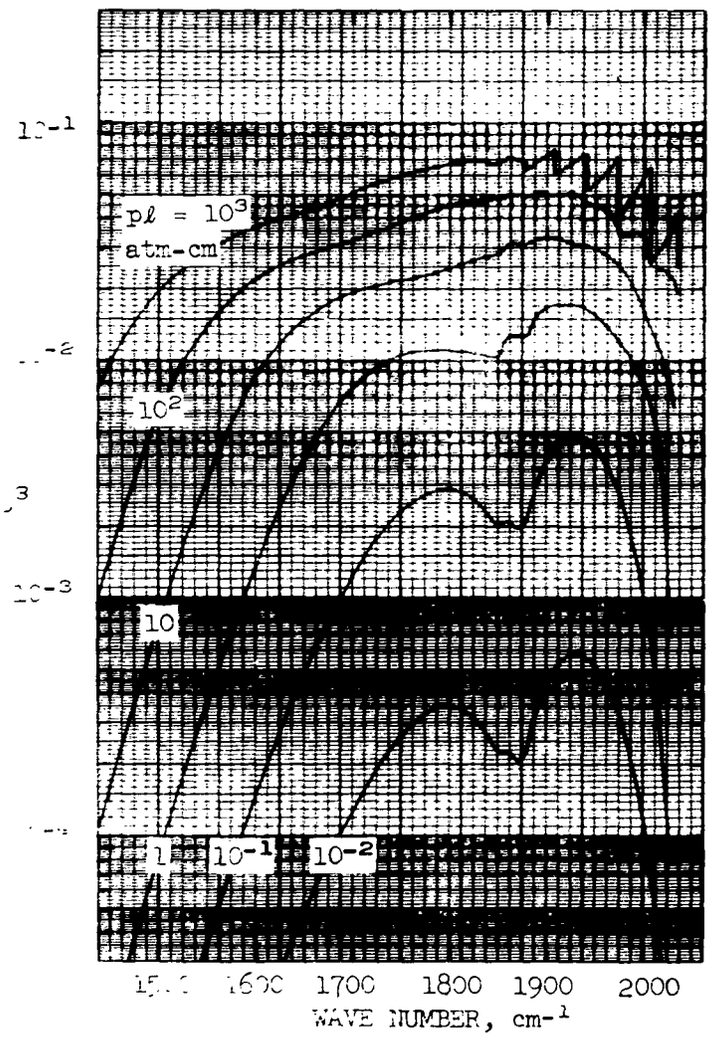

FIGURE 5. SPECTRAL EMISSIVITY OF NO AT T = 1800°K (Doppler Line Shape)

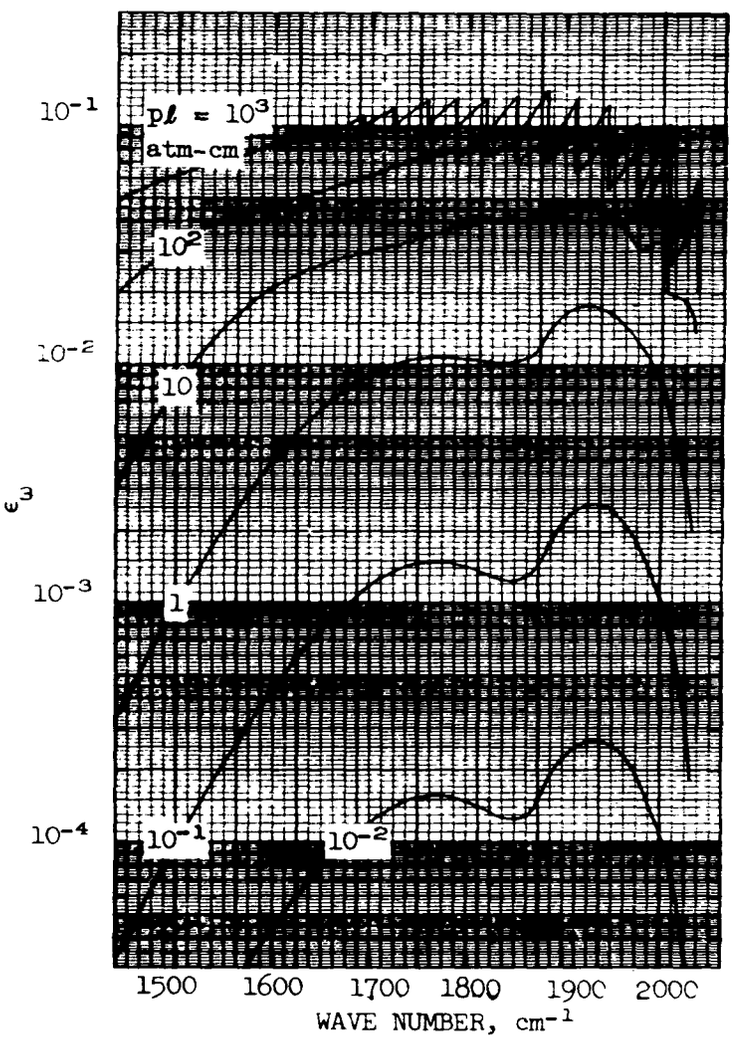

FIGURE 6. SPECTRAL EMISSIVITY OF NO AT T = 3000°K (Doppler Line Shape)

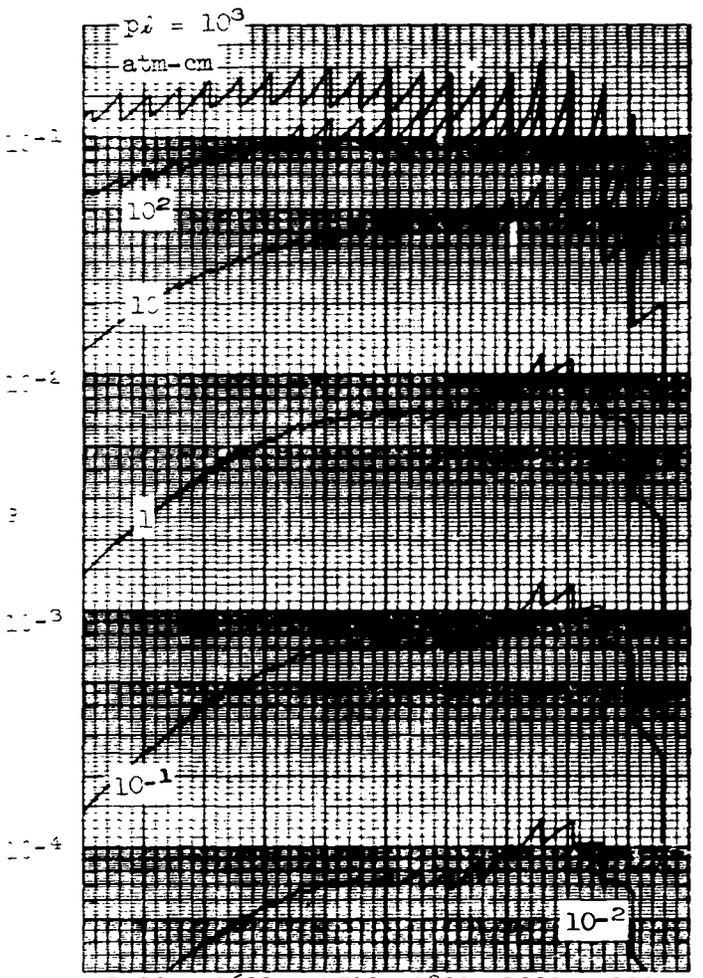

FIGURE 7. SPECTRAL EMISSIVITY OF NO AT T = 5000°K (Doppler Line Shape)

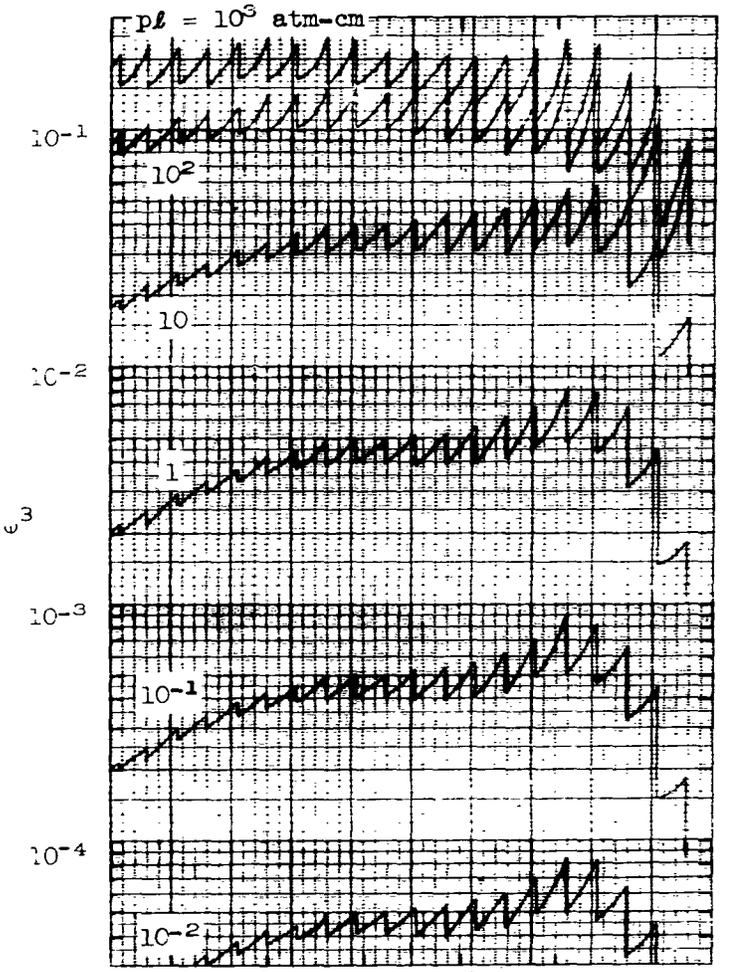

FIGURE 8. SPECTRAL EMISSIVITY OF NO AT T = 7000°K (Doppler Line Shape)

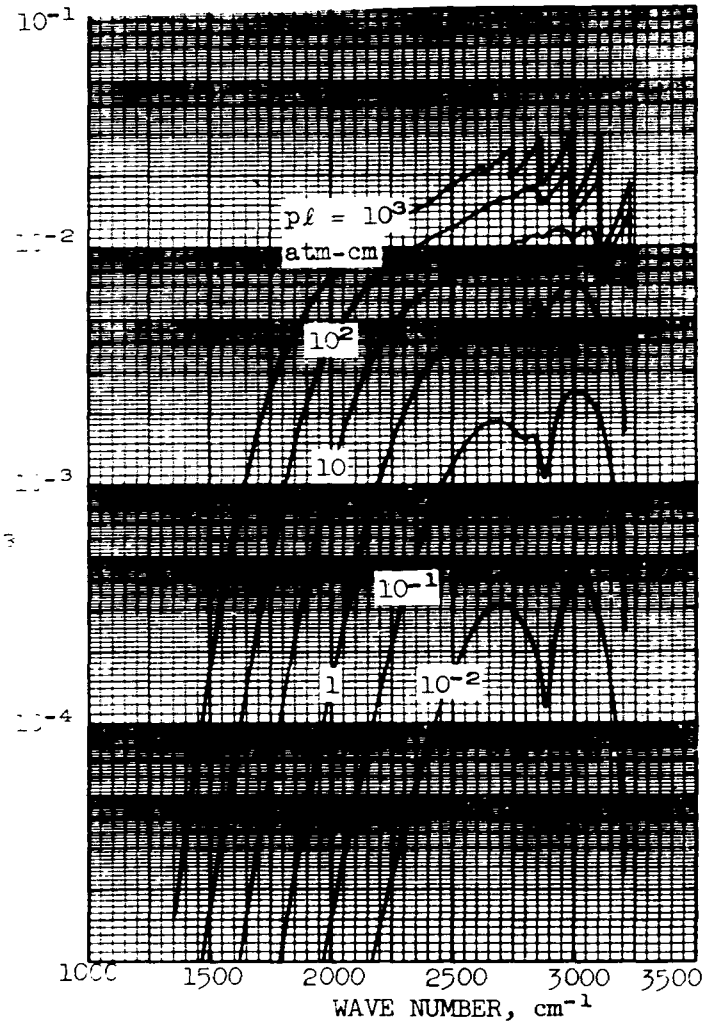

FIGURE 9. SPECTRAL EMISSIVITY OF HCℓ AT T = 1800°K (Doppler Line Shape)

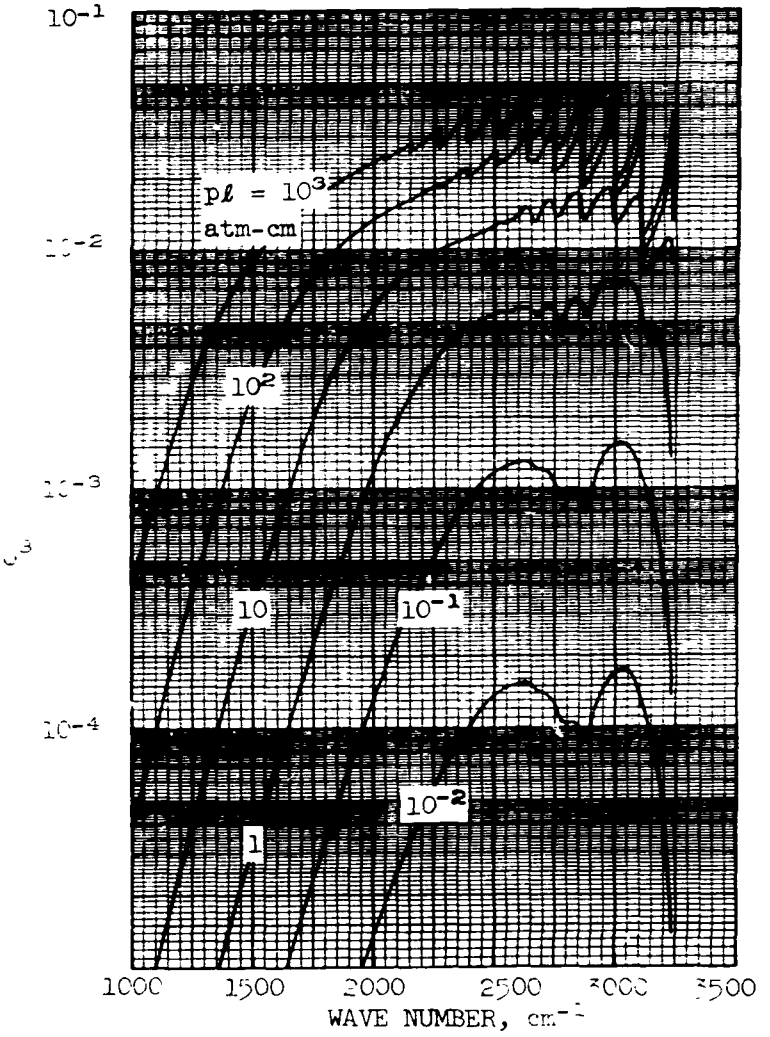

FIGURE 10. SPECTRAL EMISSIVITY OF HCℓ at T = 3000°K (Doppler Line Shape)

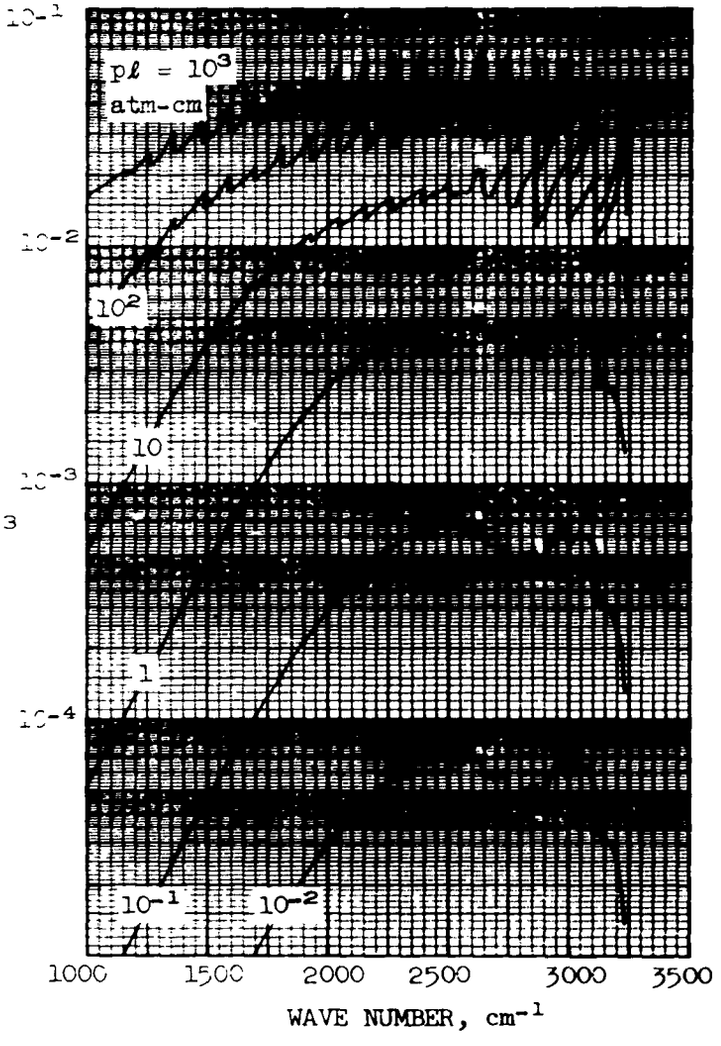

FIGURE 11. SPECTRAL EMISSIVITY OF HCℓ AT T = 5000°K (Doppler Line Shape)

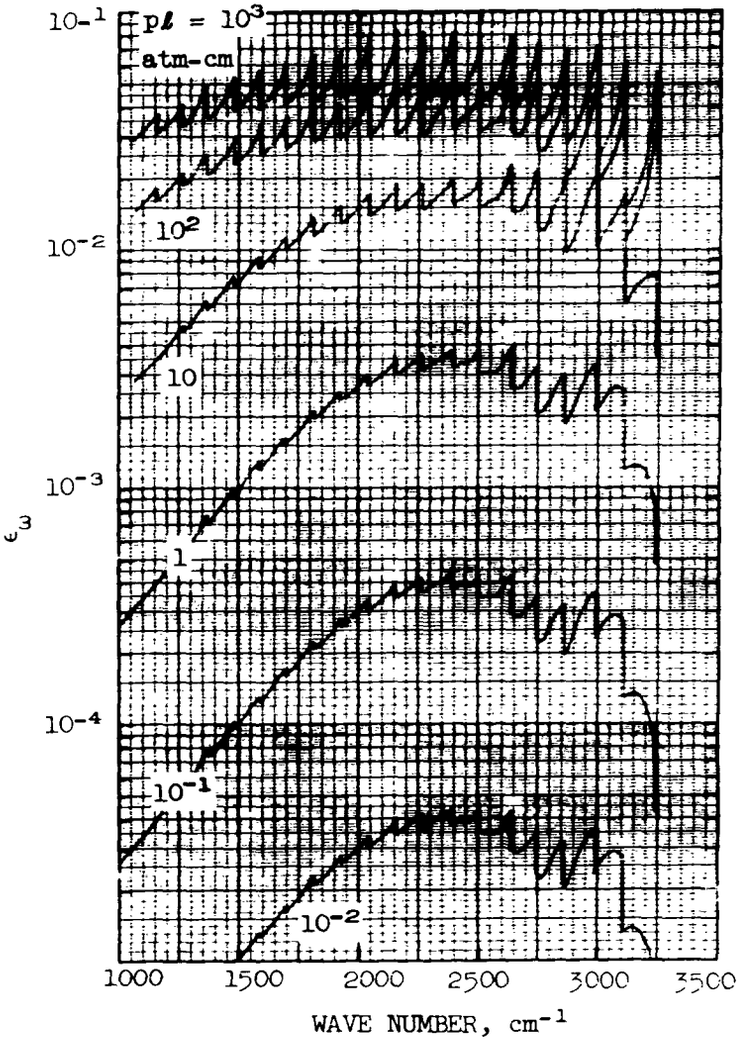

FIGURE 12. SPECTRAL EMISSIVITY OF HCℓ at T = 7000°K (Doppler Line Shape)

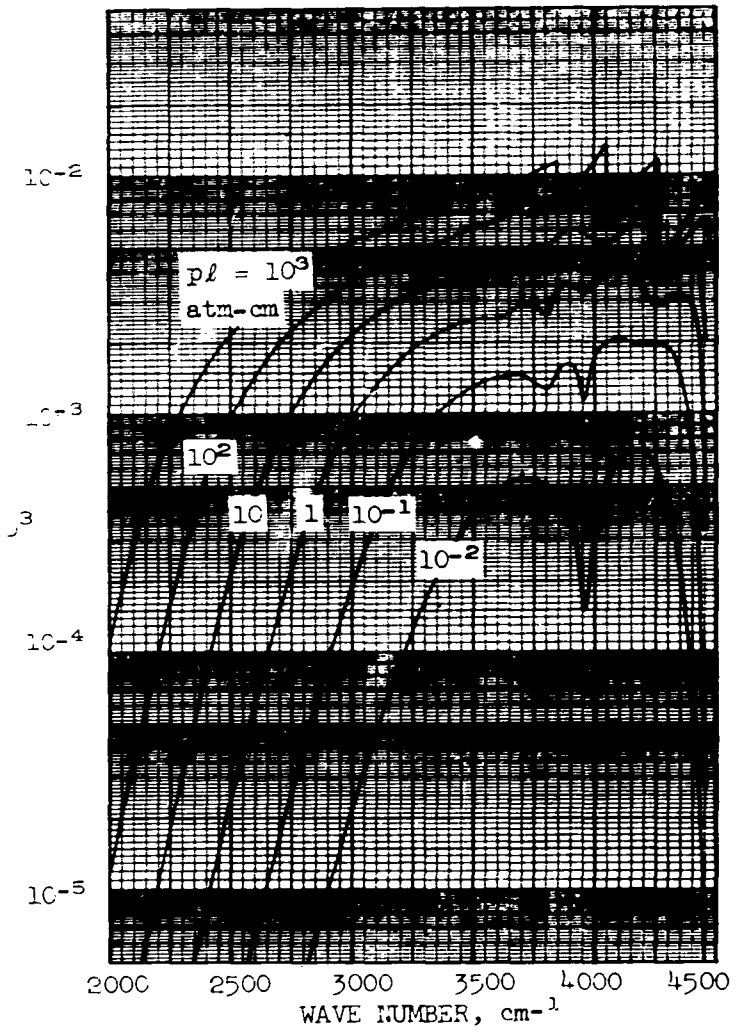

FIGURE 13. SPECTRAL EMISSIVITY OF HF AT T = 1800°K (Doppler Line Shape)

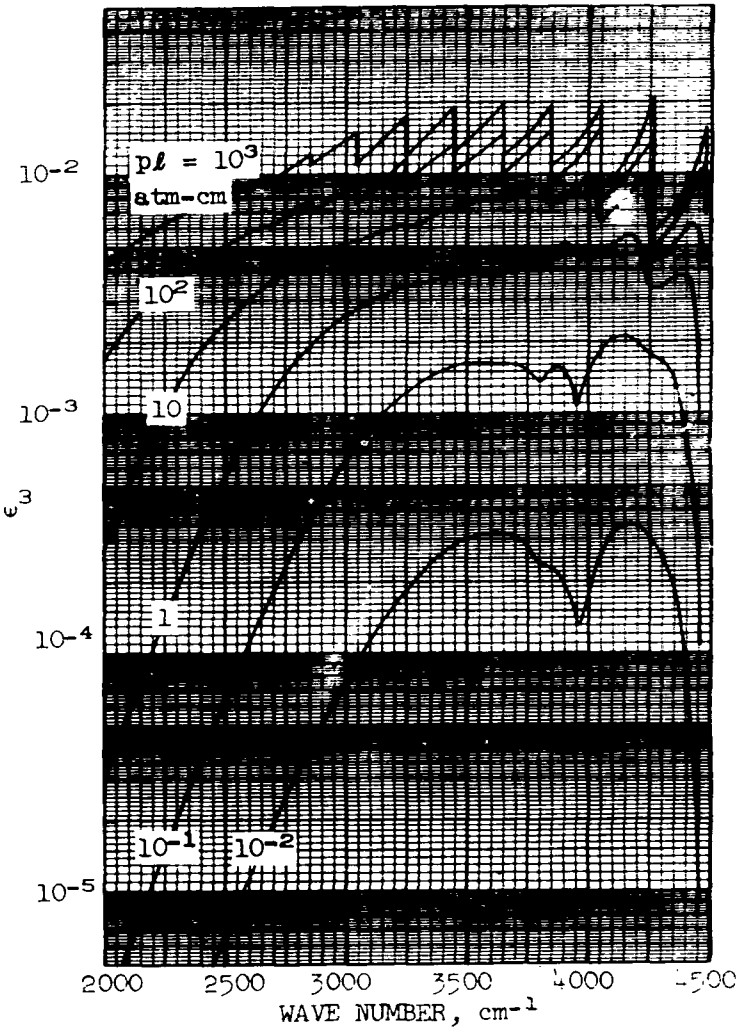

FIGURE 14. SPECTRAL EMISSIVITY OF HF AT T = 3000°K (Doppler Line Shape)

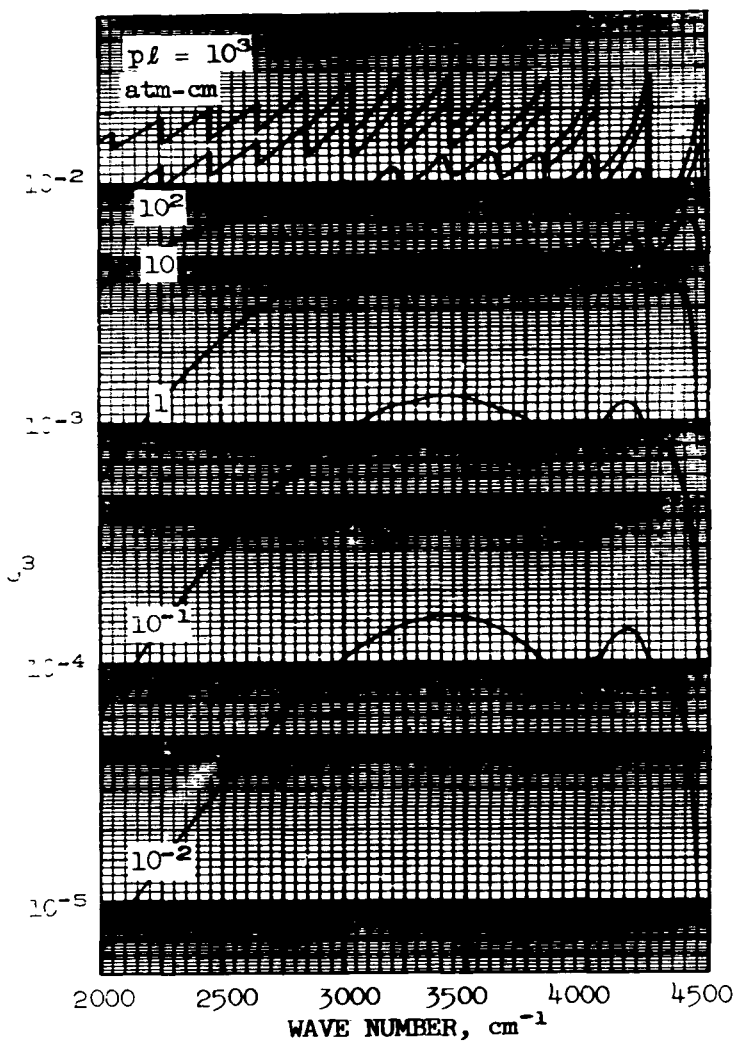

FIGURE 15. SPECTRAL EMISSIVITY OF HF AT T = 5000°K (Doppler Line Shape)

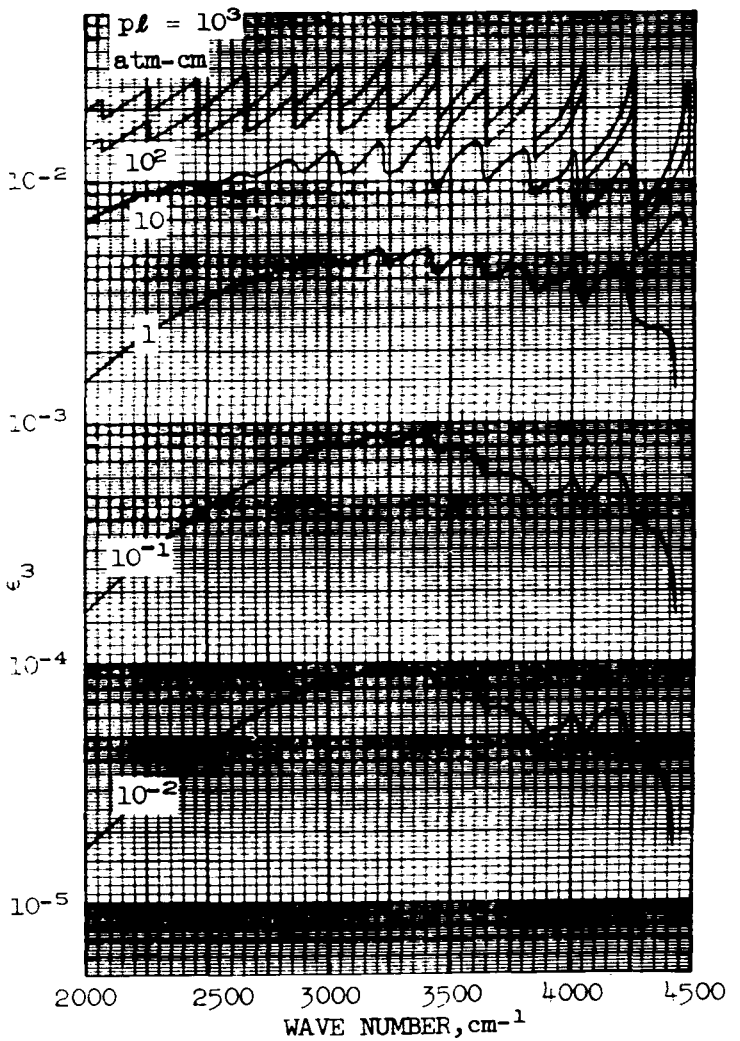

FIGURE 16. SPECTRAL EMISSIVITY OF HF AT T = 7000°K (Doppler Line Shape)

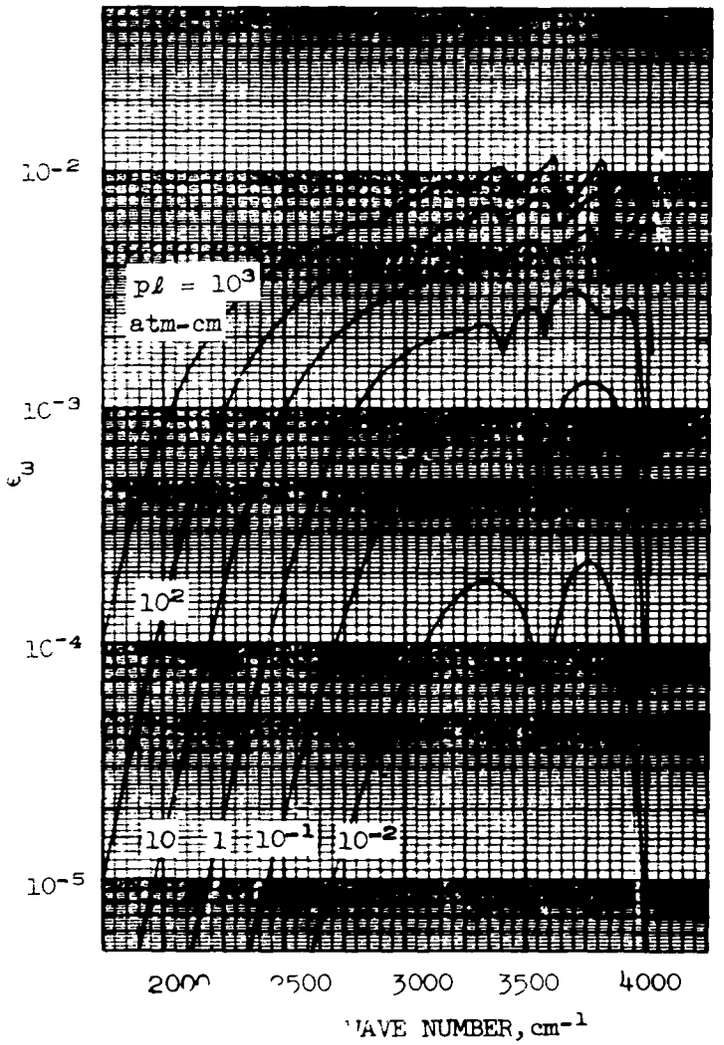

FIGURE 17. SPECTRAL EMISSIVITY OF OH AT T = 1800°K (Doppler Line Shape)

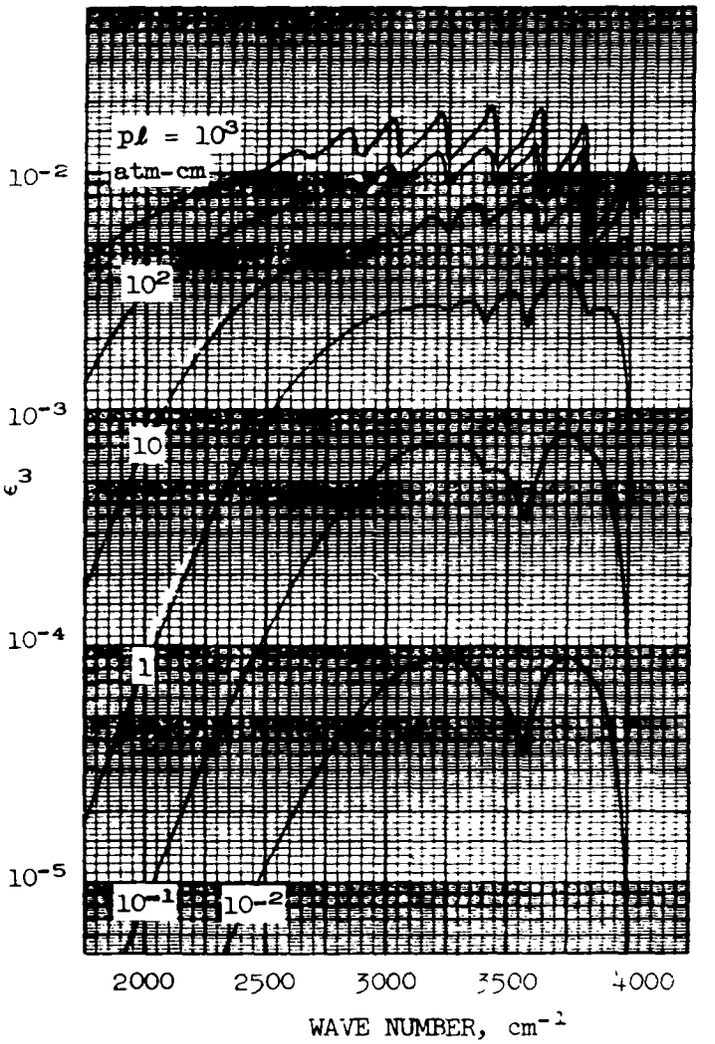

FIGURE 18. SPECTRAL EMISSIVITY OF OH AT T = 3000°K (Doppler Line Shape)

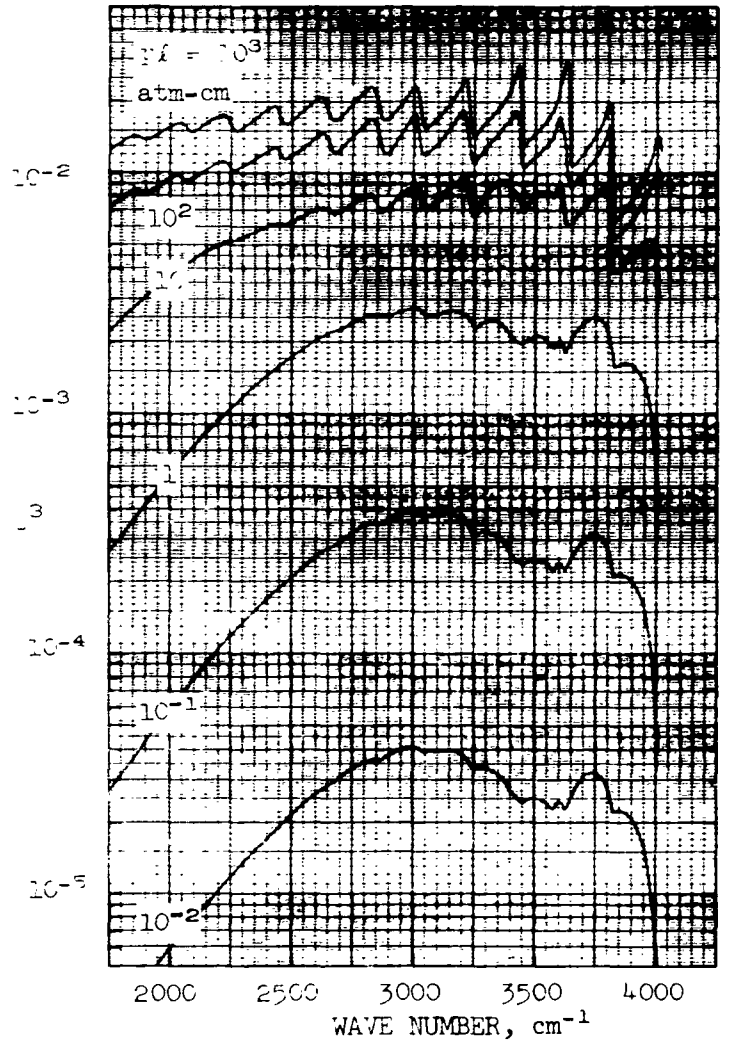

FIGURE 19. SPECTRAL EMISSIVITY OF OH AT T = 5000°K (Doppler Line Shape)

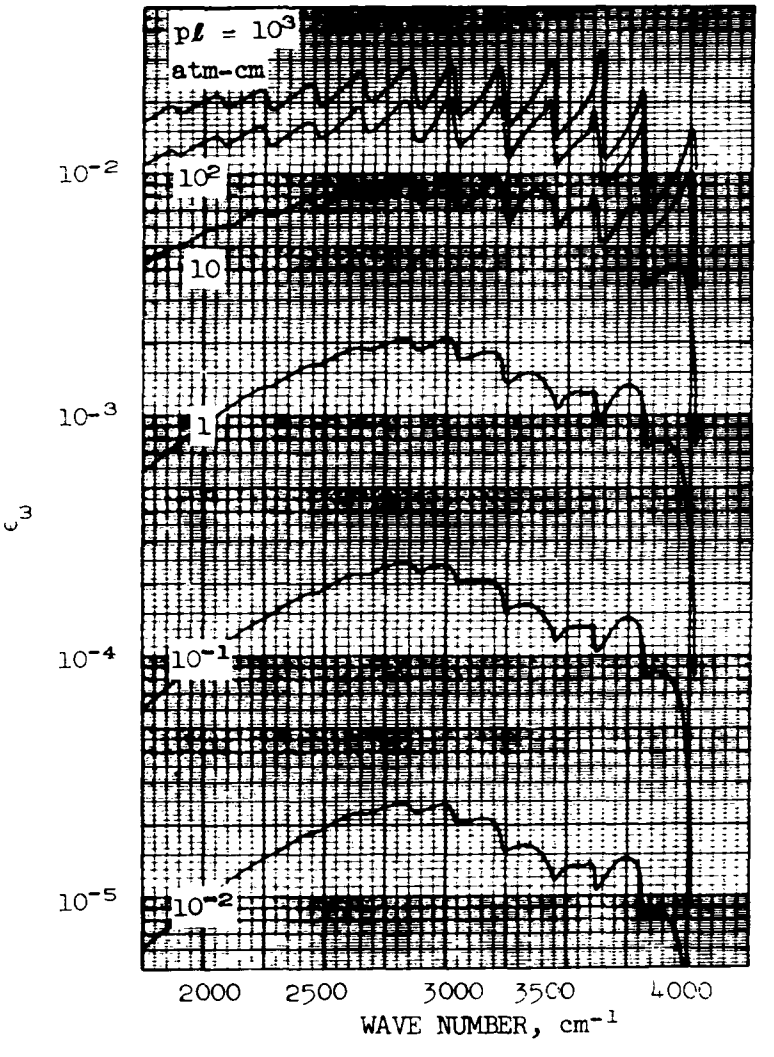

FIGURE 20. SPECTRAL EMISSIVITY OF OH AT T = 7000°K (Doppler Line Shape)